CMP Mechanisms

Mat. Res. Soc. Symp. Vol. 613 © 2000 Materials Research Society

The Effect of Wafer Shape on Slurry Film Thickness and Friction Coefficients in Chemical Mechanical Planarization

Joseph Lu[a], Jonathan Coppeta[a], Chris Rogers[a], Vincent P. Manno[a], Livia Racz[a], Ara Philipossian[b], Mansour Moinpour[b], Frank Kaufman[c]
[a]Tufts University, Dept. Mechanical Engineering, Medford, MA 02155 USA
[b]Intel Corporation, Santa Clara, CA 95052 USA
[c]Cabot Corporation, Aurora, IL 60504 USA

ABSTRACT

The fluid film thickness and drag during chemical-mechanical polishing are largely dependent on the shape of the wafer polished. In this study we use dual emission laser induced fluorescence to measure the film thickness and a strain gage, mounted on the polishing table, to measure the friction force between the wafer and the pad. All measurements are taken during real polishing processes. The trends indicate that with a convex wafer in contact with the polishing pad, the slurry layer increases with increasing platen speed and decreases with increasing downforce. The drag force decreases with increasing platen speed and increases with increasing downforce. These similarities are observed for both in-situ and ex-situ conditioning. However, these trends are significantly different for the case of a concave wafer in contact with the polishing pad. During ex-situ conditioning the trends are similar as with a convex wafer. However, in-situ conditioning decreases the slurry film layer with increasing platen speed, and increases it with increasing downforce in the case of the concave wafer. The drag force increases with increasing platen speed as well as increasing downforce. Since we are continually polishing, the wafer shape does change over the course of each experiment causing a larger error in repeatability than the measurement error itself. Different wafers are used throughout the experiment and the results are consistent with the variance of the wafer shape. Local pressure measurements on the rotating wafer help explain the variances in fluid film thickness and friction during polishing.

INTRODUCTION

Chemical mechanical planarization (CMP) is widely used in the manufacturing process of very large scale integrated (VLSI) circuits and ultra large scale integrated (ULSI) circuits. Some applications of these circuits include processor chips, RAM chips, and hard drives. The advantage of the CMP process is that both local and global planarity can be achieved. Planarity on the die level, and wafer level is even more desirable as production moves to 200 mm and 300 mm wafers. Both local and global planarity are extremely important in multilevel circuits with feature sizes smaller than 500 nm. The fine depth of focus requirements in current and future optical lithography techniques put extreme demands on the processes involved. The increased control of the CMP process allows for more efficient use of resources, and will aid in the development of future nanoscale circuit topographies.

The CMP process is widely used, yet there is only a limited understanding of the fundamental mechanisms involved. Fundamental research has been done to both experimentally understand polishing characteristics and analytically model the process involved [1,2,3]. Slurry film thickness during polishing is largely determined by how the hydrodynamic pressure and pad aesperity contact pressure equilibrate with the downforce applied. Some researchers have found that during polishing there is a vacuum created underneath the wafer and a negative vertical pad

displacement [4,5,6]. Others have found positive fluid pressure developing in the gap between the wafer and polishing pad [7]. In our experiments we have witnessed both cases. A concave wafer displays the vacuum effect, and a convex wafer develops positive fluid pressure in the gap. Frictional characteristics during polishing will depend on whether there is positive or negative (suction) pressure underneath the wafer. The frictional information can be used to determine what lubrication regime is involved [8]. Cook and Su have established that removal rate is largely dependent on the lubrication regime [9, 10]. Fluid thickness and polishing performance also vary in different lubrication regimes [11]. Sundarajann, Cook and Su have all cited that wafer curvature might be a factor in determining the lubrication regime involved, but little work has been done to study this effect partly due to the fact the wafer shape is difficult to control. Some numerical models analytically solve for the fluid depth between the wafer and pad as well as the wafer angle of attack by assuming a natural bow to the wafer [12].

In this paper, we will investigate the specific effect wafer curvature has on slurry film thickness and friction during CMP. Experiments have been conducted to examine how the slurry fluid thickness and friction changes with wafer shape and polishing parameters, such as platen speed and wafer downforce.

EXPERIMENT

Figure 1 shows the modified rotary polisher used to study slurry flow beneath the wafer. We use a Struers RotoPol-31 tabletop polisher to rotate a 300 mm (12 in) polishing pad. An industrial rated drill press capable of variable downforce (7-70 kPa +/- 1 kPa or 1-10 psi +/- 0.2 psi) via a weighted traverse replaces the standard RotoPol head. The traverse is mounted to the drill press in such a way so that the downforce applied is directly transmitted to the wafer and will not create a moment about the drill press itself. Pad conditioning can be done either in situ, during polishing, or ex situ, before and after polishing. We use a 50 mm diameter diamond grit conditioner wafer that both rotates and sweeps across the pad.

Slurry film thickness measurements are done using an optical technique known as dual emission laser-induced fluorescence or DELIF. This technique is described in detail in Coppeta and Rogers [13]. DELIF uses the fluorescence from two different commercially available dyes (mixed in with the slurry) each fluorescing at different wavelengths to measure slurry mixing, fluid depth, or fluid temperature. A complete description of these measurements can be found in our previous work [14-17]. The dyes are excited by a 100 Watt UV lamp source and we use two high-resolution 12-bit spatially aligned digital cameras to capture the fluorescence data beneath the wafer. The optics used on these cameras enable us to image an area of 2.25 cm by 3.8 cm

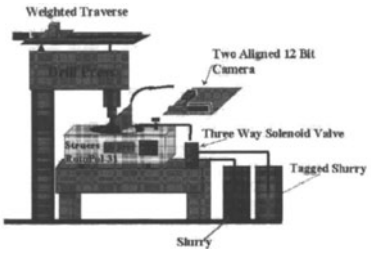

Figure 1: *Tabletop polisher and experimental Setup*

with a spatial resolution of approximately 50 µm per pixel. The images from each camera are aligned to within one pixel and can resolve fluid thickness variations down to 1 µm. Actual slurry thickness measurements are repeatable to within 5 µm. Since we are using optical techniques to measure the slurry flow beneath the wafer, actual silicon wafers cannot be used. Instead we use transparent BK-7 glass windows modified with gimbal mounts as our polishing substrates. The glass wafer is 75 mm (3 in) in diameter, and is typically bowed +/- 5 microns convex or concave. A convex wafer bows out, and a concave wafer bows in. (Figure 2 a&b)

We use a load cell mounted between two sliding plates below the polisher to measure friction during the polishing process. The bottom plate is fixed to a vibration isolation table and the polisher is fixed to the upper plate. The load cell will sense the friction force created by the interaction of the wafer and polishing pad to within 3.5% accuracy. Equation (1) shows the coefficient of friction , μ, as the friction force, F_F, normalized by the downforce, P.

$$\mu = \frac{F_F}{P} \tag{1}$$

All polishing parameters and data acquisition including platen speed, downforce, conditioner speed, and slurry flow rate are computer controlled and monitored. The cameras are similarly computer controlled and can be synchronized with changes in polishing parameters so that we can acquire image data, as well as friction data, at any point during the polishing process. The polishing parameters that we will focus on in the following results are the effects polishing pad speed and wafer downforce. The conditioner arm sweeps across the pad at 10 oscillations per minute, and the wafer rotation rate is held constant at 60 RPM.

RESULTS

This study is conducted with both in situ and ex situ conditioning. The results presented here will only include that which is done with in situ conditioning. In situ conditioning provides a more consistent pad treatment than ex situ conditioning does where pad glazing can occur. Also, the slurry film thickness referred to here is a spatially averaged measurement. Since the pad topography largely dictates how much fluid it can trap between the asperities, the fluid depth is not exactly measured from the wafer surface to the pad surface, but rather an average depth of the pad asperities. For consistent pad topography, in situ conditioning maintains these asperities and pore sizes.

The curvature of the wafer or the degree to which the wafer is bowed has a significant effect on the fluid dynamics of the polishing process. Figures 3 and 4 each correlate the trends in slurry film thickness underneath the wafer to the frictional coefficient as the polishing pad speed is changed for a convex and concave wafer, respectively. From the plot in figure 3 the slurry thickness underneath a convex wafer increases, and the coefficient of friction decreases as the pad speed increases. At a low pad velocity of 30 RPM (relative pad-wafer velocity of 0.25 m/s) the wafer rides on about a 40 µm thick slurry layer. As the pad speed increases to 90 RPM (0.72 m/s) this slurry layer increases in thickness by about 10 µm. Also, the coefficient of friction decreases about 70% over this range. This suggests that the lubrication layer between the wafer

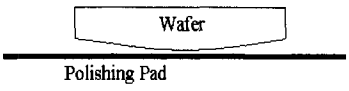

Figure 2a: *Convex wafer*

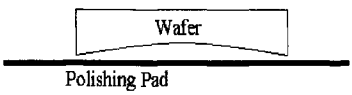

Figure 2b: *Concave wafer*

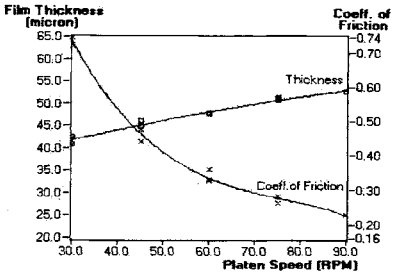

Figure 3: *Slurry film thickness and coefficient of friction as a function of pad speed for a convex wafer*

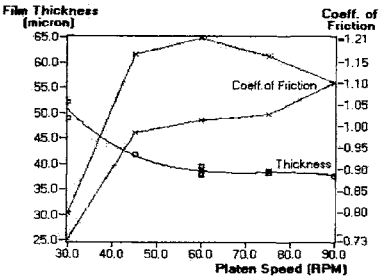

Figure 4: *Slurry film thickness and coefficient of friction as a function of pad speed for a concave wafer*

and the pad moves towards a full hydrodynamic lubrication regime at higher relative velocities, as seen previously by Coppeta et al [18]. At conditions of a full hydrodynamic lubrication regime the wafer is completely separated from the pad asperities by a fluid layer. This is in contrast to a partial or boundary lubrication regime where there is asperity contact with little or no fluid lubricating layer.

The concave wafer case is different from the previous convex wafer case. In figure 4, the slurry thickness decreases and the coefficient of friction increases as the pad speed increases. At a low pad velocity of 30 RPM the slurry film thickness is about 50 µm. As the pad speed increases to 90 RPM the slurry thickness decreases almost 15 µm. The coefficient of friction here increases 35% over the range of the same pad speeds. The trend with the concave wafer is clearly opposite from the convex. As the relative velocities increase, the concave wafer moves towards increased asperity contact meaning partial or total boundary lubrication. We have measured a net negative fluid pressure underneath the wafer for a concave wafer only. This suction brings the wafer and pad into contact, thereby, decreasing slurry thickness and increasing friction as seen by Tichy et al.

In order to isolate the effect of wafer downforce, the pad velocity is fixed at 60 RPM (relative wafer-pad velocity of 0.5 m/s) and the applied downforce is varied from 2 psi to 6 psi. In both cases of convex and concave wafers, the slurry film thickness decreases about 15 µm for a 4 psi increase in downforce. Although the trends are the same, the slurry layer thickness under the convex wafer is about 10 µm greater than that for the concave wafer. The manner in which

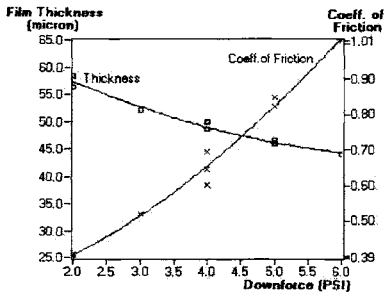

Figure 5: *Slurry film thickness and coefficient of friction as a function of downforce for a convex wafer*

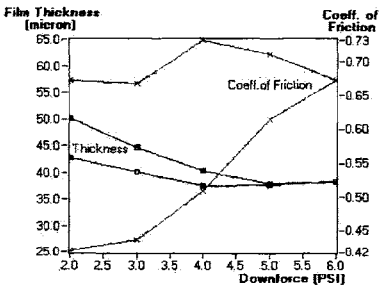

Figure 6: *Slurry film thickness and coefficient of friction as a function of downforce for a concave wafer*

the pad conforms to the wafer shape is believed to be one of the causes of this difference. The increased wafer downforce pushes the wafer into the compliant pad creating higher pad asperity pressure and decreasing relative fluid pressure. Therefore, less slurry resides in the gap between the wafer and the pad.

However, the behavior of the slurry film thickness and the coefficient of friction in the concave wafer case is not what we would expect. The expectation of the thickness and friction for the concave wafer in figure 6 would be the same trends as the convex wafer's in figure 5. From figures 4 and 6 the repeatability in the data of the concave wafer is compromised for two reasons. The wafer is polishing, therefore changing shape during this experiment, and the pad is deforming as well. In figure 6, as the downforce is decreased from 6 psi to 2 psi the slurry thickness increases to 50 μm, higher than it was originally (43 μm), at 2 psi. This experimental phenomenon has been repeated over a range of input parameters and at this time a possible explanation for this repeatable experimental result could be the effects of hysterisis in pad compliance. It will be necessary to understand the pad's response to changing downforce not only to characterize the lubrication regime, but also to understand how the pad preferentially polishes fine features on a patterned wafer.

The coefficient of friction, in figure 6, drops as the downforce reaches 6 psi and then continually decreases as the downforce is reduced back down to 2 psi. As the wafer goes from concave to increasingly convex the lubrication regime during polishing changes. As seen earlier, a convex wafer sees a far greater amount of hydrodynamic lubrication than a concave wafer. So as this experiment progresses the level of hydrodynamic lubrication increases, the frictional coefficient decreases, and the slurry thickness increases as the wafer hydroplanes. To truly isolate the effect of wafer shape the concavity of the wafer needs to be preserved.

Another way to look at the fluid dynamics between the wafer and polishing pad is to consider at the wafer angle of attack, or wafer tilt angle. We measure the fluid thickness under the front half and back half of the wafer and extrapolate the angle of attack from the difference in thickness. This technique can accurately measure angle of attack down to 0.003 degrees. Figure 7 is a comparison of this tilt angle as a function of wafer downforce for a convex and concave wafer. The angle of attack for a convex wafer is greater by orders of magnitude than that of a concave wafer. As the wafer downforce increases the convex wafer's angle of attack decreases, whereas the concave wafer's angle of attack relatively does not change. The substantially greater angle of attack of the convex wafer can continually support a larger hydrodynamic fluid layer. In the other case where the concave wafer's angle of attack is low, it becomes difficult for the wafer to maintain a hydrodynamic fluid layer.

CONCLUSION

The wafer curvature strongly affects the fluid behavior during CMP. We have examined

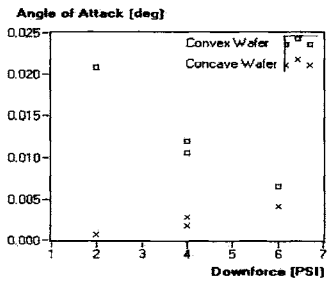

Figure 7: *Wafer angle of attack as a function of downforce*

both convex and concave wafers and their effects on slurry film thickness and the coefficient of friction. A convex wafer is found to support a hydrodynamic fluid layer much more easily than a concave wafer. As the relative pad-wafer velocity increases a convex wafer will ride on an increasingly thick slurry film, whereas a concave wafer will be sucked into the polishing pad increasing asperity contact and friction. As wafer downforce increases the slurry film thickness decreases. In this case the wafer shape determines the relative thickness of the slurry layer. The shape of the wafer has a large influence on the lubrication regime that exists between the wafer and polishing pad. In order to further understand the correlation between slurry film thickness and friction, additional knowledge of the polishing pad's response to pressure fluctuations is necessary. Through some accurate measurements of friction and slurry layer thickness during CMP, increased control of the process may lead to greater polishing performance.

ACKNOWLEDGEMENTS

The authors would like to thank Intel and Cabot corporations for funding this research. We would like to thank VEECO corporation for the donation of a Dektak 200 Si profilometer that enabled us to measure wafer topographies. We would also like to thank Freudenberg Nonwovens for donating FX-9 polishing pads.

REFERENCES

1. L. Cook, J. Non-Crystalline Solids **120**, 152-171 (1990).
2. Z. Stavreva, D. Zeidler, M. Plotner, K. Drescher, App. Surf. Sci. **108**, 39-44 (1997).
3. S. Runnels, J. Electrochem. Soc. **141**, 1900-1904 (1994).
4. J. Levert, R. Baker, F. Mess, R. Salant, S. Danyluk, STLE Trib. Trans., Submitted for publication Aug. 1997.
5. F. Mess, J. Levert, S. Danyluk, Wear **211**, 311-315 (1997).
6. J. Tichy, J. Levert, L. Shan, S. Danyluk, J. Electrochem. Soc. **146**, 1523-1528 (1999).
7. S. Sundararajan, D. Thakurta, D. Schwendeman, S. Murarka, W. Gill, J. Electrochem. Soc. **146**, 761-766 (1999).
8. J. Lu, J. Coppeta, C. Rogers, L. Racz, A. Philipossian, F. Kaufman, J. Electrochem. Soc. (submitted Nov.1999).
9. L. Cook, J. Wang, D. James, A. Sethuraman, Semiconductor Int'l. Nov. 1995, 141-144.
10. Y. Su, S. Wang, J. Hsiau, Wear **188**, 77-87 (1995).
11. M. Bhushan, R. Rouse, J. Lukens, J. Electrochem. Soc. **142**, 3845-3851 (1995).
12. S. Runnels, L. Eyman, J. Electrochem. Soc. **141**, 1698-1701 (1994).
13. J. Coppeta, C. Rogers, Experiments In Fluids 25, 1-15 (1998).
14. C. Rogers, J. Coppeta, L. Racz, A. Philipossian, F. Kaufman, D. Bramono, J. Elec. Mat. **27**, 1082-1087 (1998).
15. J. Coppeta, C. Rogers, L. Racz, A Philipossian, F. Kaufman, Proc. CMP-MIC Conf., Santa Clara, CA, 1999.
16. J. Coppeta, L. Racz, C. Rogers, A. Philipossian, F. Kaufman, Int'l J. of CMP for On-Chip Interconnection **1**, 47 (1999).
17. J. Coppeta, C. Rogers, L. Racz, A. Philipossian, F. Kaufman, J. Electochem. Soc. **147** (to be published May 2000).
18. J. Coppeta, J. Lu, D. Bramono, C. Rogers, L. Racz, A. Philipossian, F. Kaufman, 4th Int'l Symposium on CMP, Lake Placid, New York, Aug 8-11, 1999.

Mat. Res. Soc. Symp. Vol. 613 © 2000 Materials Research Society

A MODEL OF CHEMICAL MECHANICAL POLISHING

Ed Paul Stockton College, Pomona NJ 08240 and NIST, Gaithersburg MD 20899 U.S.A.

ABSTRACT

A generic model is presented which explains the dependence of chemical mechanical polishing rates on the concentration of reacting chemicals and abrasives in the slurry. The predictions of this model are compared to data from the literature for tungsten CMP.

INTRODUCTION AND THEORY

CMP has been described qualitatively as an alternation of chemical reaction and mechanical abrasion processes[1]. This paper provides a generic, semiquantitative description for both of these processes and links these descriptions to form a model that predicts the removal rate as a function of the concentrations of chemicals and abrasives in the slurry. Certain modifications are needed to apply the generic model to specific systems. As an example, the results will be compared to polishing data available in the literature for tungsten.

In this model of CMP, the abrasive particles are small and the pad and slurry fluid support the load. Chemical reactions between the workpiece material and chemicals in the slurry form a thin film on the workpiece surface. This film, which is not tightly bonded to the bulk material, is separated from the workpiece surface by abrasive particles, which are pushed into it by the polishing pad. Fresh surface is then exposed on the workpiece, and this surface is available for reaction with the chemicals in the slurry for a subsequent CMP cycle. The chemical process of forming the reaction surface film depends on how much of the reacting chemical is in the slurry. At low chemical concentrations, the surface is only partially covered. Increases in chemical concentration will increase the surface coverage until the film is complete and additional chemical has no effect on the polishing rate. Similarly, the mechanical process of removing this film depends on the amount of abrasive in the slurry. At high abrasive loading, the pad is full and adding more abrasive will not affect the polishing rate, while at low abrasive loading there is space on the pad surface to hold more abrasive particles. In this case, additional abrasive will increase the polishing rate. A quantitative discussion of these processes is presented below.

Chemical Reaction Process In the chemical process, the workpiece material reacts with chemical components of the slurry to form a thin reaction film. This surface reaction is subject to the laws of chemical equilibrium, and can be written schematically as

$$M + C \rightleftharpoons MC^* \qquad \text{Rxn. 1}$$

where M and C represent the workpiece material M and the reacting chemical C while MC* represents the surface complex which forms the film. The reaction is a reversible one: the film can decompose and return chemical C to the slurry. The MC* complex is available for either dissolution into the slurry or for mechanical abrasion. When stable surface films form, their dissolution, sometimes called corrosion, is a slow process. It may be written as

$$MC^* \rightarrow MC_{(aq)} + M \qquad \text{(Rxn. D)}$$

where MC*(aq)* represents the product dissolved into the slurry and M is the workpiece surface material, revealed when the surface complex is removed. The abrasion step may be written as

$$MC^* + A \rightarrow MC\text{-}A + M \qquad \text{(Rxn. M)}$$

for abrasive particles A, with material MC-A leaving the workpiece surface to expose fresh M.

Chemical kinetics predicts rates using rate constants for simple reactions. In this case, reversible reaction 1 has associated rates for the forward (f) and reverse (r) reactions

$$r_{1f} = k_{1f}\, N_M\, [C] \qquad (1f)$$
$$r_{1r} = k_{1r}\, N_{MC^*} \qquad (1r)$$

where k_i is the rate constant for reaction i, N_M and N_{MC^*} are the number of M and MC* sites on the workpiece surface, and [C] is the concentration of reacting chemical in the slurry. The rate for dissolution is proportional to N_{MC^*} while the rate for mechanical abrasion depends on both N_{MC^*} and the number of effective abrasive particles N_A per area **A**.

$$r_D = k_D\, N_{MC^*} \qquad (2)$$
$$r_M = k_M\, (N_A/\mathbf{A})\, N_{MC^*} \qquad (3)$$

The total removal rate is the sum of these corrosion and abrasion rates, and is proportional to the number of surface complexes N_{MC^*}. Standard methods of chemical kinetics for surface reactions show that the rate of change of N_{MC^*} is

$$d\, N_{MC^*}/dt = k_{1f}\, N_M\, [C] - k_{1r}\, N_{MC^*} - k_D\, N_{MC^*} - k_M\, (N_A/\mathbf{A})\, N_{MC^*} \qquad (4)$$

which equals 0 at steady state, when the rate of formation of MC* balances the rate of removal. The total number of surface sites N_{oM} is related to the workpiece area **A** by the area per site, d_M^2.

$$N_{oM} = N_M + N_{MC^*} = \mathbf{A}/d_M^2 \qquad (5)$$

At steady state, combining Eqs. 4 and 5 gives

$$N_{MC^*} = (N_{oM})\, [C] / ([C] + (k_{1r} + k_D + k_M(N_A/\mathbf{A}))/ k_{1f}) = (\mathbf{A}/d_M^2)\, \theta \qquad (6)$$

where $\theta = N_{MC^*}/N_{oM}$ is the fraction of surface sites covered by the MC* complex. This expression will be used to find the polishing rate in Section IV.

Mechanical Abrasion Process The mechanical abrasion rate depends on the number of effective abrasive particles in the slurry that are available for contact with the workpiece. In this model, the polishing pad has a limited total number of surface sites, N_{oP}, which hold abrasive particles. At any given concentration of abrasive, some of these sites will be occupied and others will be empty. The fraction of occupied sites depends on the abrasive concentration: Let r_{Af} be the rate at which an abrasive particle enters a pad site from the slurry. This is proportional to the number of available sites N_s, the concentration of abrasives in the slurry [A], and the rate constant k_{Af} giving $r_{Af} = k_{Af}\, N_s\, [A]$. The rate at which abrasives leave the pad is proportional to the number of occupied sites N_A, so $r_{Ar} = k_{Ar}\, N_A$. The total number of sites on a pad may be written as $N_{oP} = N_s + N_A$. At steady state, the forward and reverse rates balance. Combining these equations gives N_A, the number of effective abrasives on pad area **A**.

$$N_A = N_{oP}\, [A] / ([A] + (k_{Ar}/k_{Af})) = \mathbf{A}\, c_P\, [A] / ([A] + K_A) = \mathbf{A}\, c_P\, \theta_A \qquad (7)$$

where $c_P = N_{oP}/\mathbf{A}$ is the site density on the pad, $K_A = (k_{Ar}/k_{Af})$ is the pad-abrasive equilibrium constant, and θ_A is the fraction of pad sites occupied by abrasive particles.